

Investigation on blade angles effect on micro-gravitational water vortex system via simulation and experimental analysis

Wong Kee Seng¹, Shirley Johnathan Tanjong^{1,*}

¹ Department of Mechanical and Manufacturing Engineering, Faculty of Engineering, Universiti Malaysia Sarawak, 94300 Kota Samarahan, Sarawak, Malaysia

ARTICLE INFO

Article history:

Received 16 December 2024

Received in revised form 16 January 2025

Accepted 20 February 2025

Available online 31 March 2025

Keywords:

Simulation; Computational Fluid Dynamics; micro gravitational water vortex; Kaplan turbine; blade angle; green energy

ABSTRACT

Micro gravitational water vortex power plants offer a promising solution for generating electricity from renewable energy sources with minimal hydraulic pressure requirements. Increased energy generation results from an increased vortex formation. Thus, the design of a micro gravitational water vortex system aims to achieve a powerful artificial air-core vortex. This study focused on investigating the effect of different blade angles in a Kaplan turbine within a micro gravitational water vortex system. Computational fluid dynamics (CFD) simulations conducted using Ansys software provided detailed insights into fluid flow dynamics, while experimental validation of the numerical results involved computational design and modelling, fabrication of the blades prototype on a 3D printer, and experimental data collection. Three blade angles at 140°, 150°, and 160°, were examined to determine its effects on power efficiency, approximate power input, and output. Simulation results indicate that a blade angle of 140° yields the highest power efficiency, reaching an impressive value of 95.40%. This efficiency outperforms the other blade profiles investigated. Experimental results showed reasonable consistency with the numerical predictions, with errors between numerical and experimental value ranging from 4.5% to 27.6%. Findings presented in this paper emphasised the importance of blade angle selection in optimizing the performance of micro gravitational water vortex power plants. Valuable insights for the design and operation of this eco-friendly technology aid the advancement of green energy generation systems.

1. Introduction

Malaysia has made significant progress in rural development, particularly in lowering poverty rates and improving quality of living by expanding electricity supply. To increase its economic competitiveness and resilience, Malaysia is developing its power supply with an emphasis on guaranteeing a secure, dependable, and cost-effective supply of energy. At the same time, the country is ardent in advocating the efficient use of energy resources and the usage of energy, especially renewable energy.

* Corresponding author.

E-mail address: jtshirley@unimas.my

<https://doi.org/10.37934/pjfd.1.1.1327>

To enhance the standard of living in rural communities, the execution of the rural electrification program had stepped up in the 9th Malaysian Plan, particularly in remote areas of Sarawak. To increase electricity supply to these areas, the government is sponsoring the rural electrification program by installing Micro Gravitational Water Vortex Power Plant (MGWVPP) at Sarawak's rural areas [16]. MGWVPP uses renewable energy sources to produce electricity. MGWVPP is a vortex power plant which creates free water vortex. Free water vortex transfers tangentially into the water basin and a turbine is then used to extract energy from the free vortex. The primary advantages of this form of power plant are its capability to produce electricity using very low hydraulic pressure and its environmental friendliness. MGWVPP can operate with a minimum hydraulic head requirement as low as 1m, thus can be built close to a riverbank or a stream to provide electricity for a few residences [8].

The concept of MGWVPP is new, with limited research available on this topic [5,9]. An earlier study investigated Francis turbine, Propeller and Kaplan turbine, pump as turbine and vortex water turbine for micro hydro system [9]. Due to the way the vortex movement moves tiny solid particles through the turbine, micro hydro system can tolerate muddy and unclean water. A study found that turbine effectiveness improved when the turbine blade is twisted [16]. Study by Dhakal *et al.* [3], Nishi *et al.* [7] and Sanchez *et al.* [10] compared different basin geometries of the micro hydro system. Thus, there are opportunities to explore ways to improve a MGWVPP design.

Therefore, the main aim of this study was to design and investigate the performance of three different shapes of the turbine's blade. To achieve the aim of the project, we detailed the objectives as follows:

- a) Objective 1 - to design and simulate different curved angle of Kaplan turbine blade i.e., 140°, 150° and 160° blade angle in 3D drawing using SolidWorks and Ansys.
- b) Objective 2 - to compare performance of three different blade angle of turbine i.e., 140°, 150° and 160° based on CFD simulation.
- c) Objective 3 - to fabricate the three different blade angle of turbine blades by using 3D printer and assemble a prototype of micro gravitational water vortex plant.
- d) Objective 4 - to compare power efficiency of the prototype and simulation model of micro gravitational water vortex plant.

2. Background Review

2.1 Micro-Gravitational Water Vortex Power Plant (MGWVPP)

Micro-gravitational water vortex power plant is a small-scale hydropower plant. The system uses the hydropower as the driving force to generate the electricity. Micro hydropower is classified as the size of 200 kW which differs from a typical hydroelectric power plant, particularly in the amount of energy generated [12]. The very basic equipment and restricted space needed for micro hydro installation and operation are a result of the relatively low energy output of the technology when compared to large-scale hydropower. One benefit of micro hydropower system is that, it does not harm the environment. Therefore, the micro hydropower system is excellent for connecting electrical energy networks in rural and isolated locations that cannot be serviced by power companies like Sarawak Energy in Malaysia. It is normally built at small streams and natural waterfalls. MGWVPP has an extraordinarily low head of 0.7–3 m and can produce renewable energy that is absorbed by high-quality, environmentally friendly output [12]. In general, the micro-gravitational water vortex power plant is made up of three main components which are turbines, generator, and cylindrical basin.

The operational mechanism of the power plant involves the conversion of water flow's potential energy into electrical energy. This potential energy arises from the water flowing from a certain height difference. The process begins with water being fed tangentially into a basin via a large inlet channel, creating a water vortex. At the bottom of the basin, water passes through an exit hole through which the water is discharged. The water vortex will rotate the turbine's blade and the produced rotational motion will be connected to a shaft connects to a generator. Instead of using pressure differential to produce torque on the output shaft, the vortex turbine uses the dynamic force of the vortex over the turbine runner [5,9]. The gravitational potential of the water that can be transformed into electrical energy increases with the water head drop.

2.1.1 Head

The head of micro hydro system can be classified into two types which are high head and low head. Presently, high head impulse type turbines like Pelton turbine and crossflow turbine are used often in commercialized medium hydro plant. Since pressurised water from the head is used to create power rather than flow rate, these impulse type turbines are more often employed in high head medium hydro systems than reaction turbines. They are also less expensive and smaller. However, flat locations with a larger resident density are suited for low head micro hydro. Low head micro hydro systems sometimes demand more costly, larger equipment and specialist technical input to enable implementation. As a result, low head micro hydro applications in rural locations are uncommon, and there is little information accessible for potential customers [15]. The hydraulic head requirement of MGWVPP is ultra-low because it relies on the dynamic force produced by the vortex rather than the pressure differential to operate.

2.1.2 Inlet and outlet valve

Water released into a channel that is connected to the basin is the MGWVPP's input flow rates. The channel, which can be flat or inclined at an angle, guide water to flow into a basin. Cylindrical basin with a discharge hole produces a higher and more predictable velocity than conical basin and rectangle basin [16]. Channel width might vary or remain constant between two ends [9]. Inlet height can be referred as: (i) height of the water, and (ii) height of the channel relative to the basin's bottom end. A higher basin results in higher outlet velocity [8]. The outflow is often located at the central region of the basin, and its diameter had a considerable impact on the vortex's intensity and vortex turbine's effectiveness. Shabara *et al.* [11] showed that the outlet diameter, which varies between 0.20 and 0.35 metres, significantly affects power production with a 30% total efficiency. Further, a simulation work demonstrated an inverse relationship between the output speed and outlet diameter [9]. Figure 1 shows the inlet and outlet parameters.

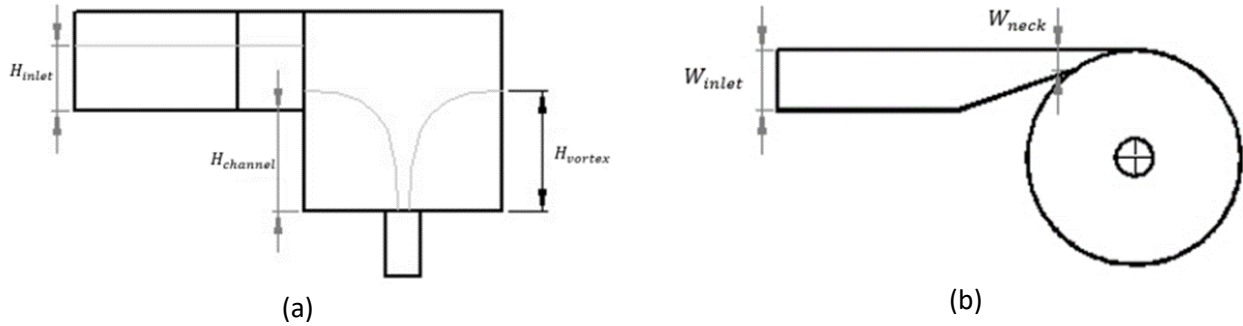


Fig. 1. Multi-gravitational water vortex power plant (a) side view, and (b) top view [9])

2.1.3 Turbine

Turbine is the most important part in MGWVPP. It is installed in the middle and lined up with basin's main exit. The waterpower from the water vortex is used to drive the turbine. Turbine converts the energy of moving water into shaft power. The pressure head available and the design flow for the planned hydropower plant will be the key determining factors in the turbine selection. Generally, water turbines can be classified into two categories which are impulse turbine and reaction turbine. In this research, we focused on Kaplan turbine, which is a type of reaction turbine. Kaplan turbine is typically used in micro hydro power generation system [2,6]. It is appropriate for use on rivers and can work at low head and high flow rates. Sritram and Suntivarakorn [13] demonstrated that the water turbine's efficiency is influenced by the number of blades. Since the space between the blades was effective for absorbing the force of the water flow on the blades, it was established that the five-bladed water turbine was the most practicable for use and generated the highest torque.

3. Methodology

Computational-aided design (CAD) of the basin and 3 different turbine blade angles i.e. 140° , 150° and 160° using Solidworks. Simulation of the 3 different blade angles fluid dynamics was done using Ansys Fluent. The scaled-down model of the MGWVPP was 3D-printed using Ender-5 Plus 3D printer with PETG filament. The prototype design was then validated by comparing the simulation results (scaled-down model) and the experimental results.

3.1 CAD of the Cylindrical Basin

Figure 2 shows the cylindrical basin design. The cylindrical basin was designed with a discharge hole at the bottom of the cylindrical basin. This design allows generation of water vortices along with tangential water entering the basin. Water in a vortex basin flows tangentially rather than axially as its mean tangential velocity rises. This causes the height of the vortex to rise as well, enhancing the vortex [4]. Emphasis was placed on constructing a basin that produces a free surface air core vortex with the optimal height and higher velocities at the vortex's centre. Two sizes of basin were modelled i.e. the actual size model (proposed size for installation at actual site) and the scaled-down model (size of the prototype built in this study), dimensions as summarised in Table 1.

Table 1
 Dimensions of the cylindrical basin

Parameters	Actual Size (mm)	Scaled-down Size (mm)
Basin diameter	220	110
Basin height	200	100
Inlet height	50	25
Inlet width	180	90
Outlet height	50	25
Outlet diameter	50	25

The dimensions of the cylindrical basin such as basin diameter, inlet height and width, channel height, outlet diameter and height, are the same with varying turbine blade angles of 140°, 150° and 160°, as shown in Figure 2.

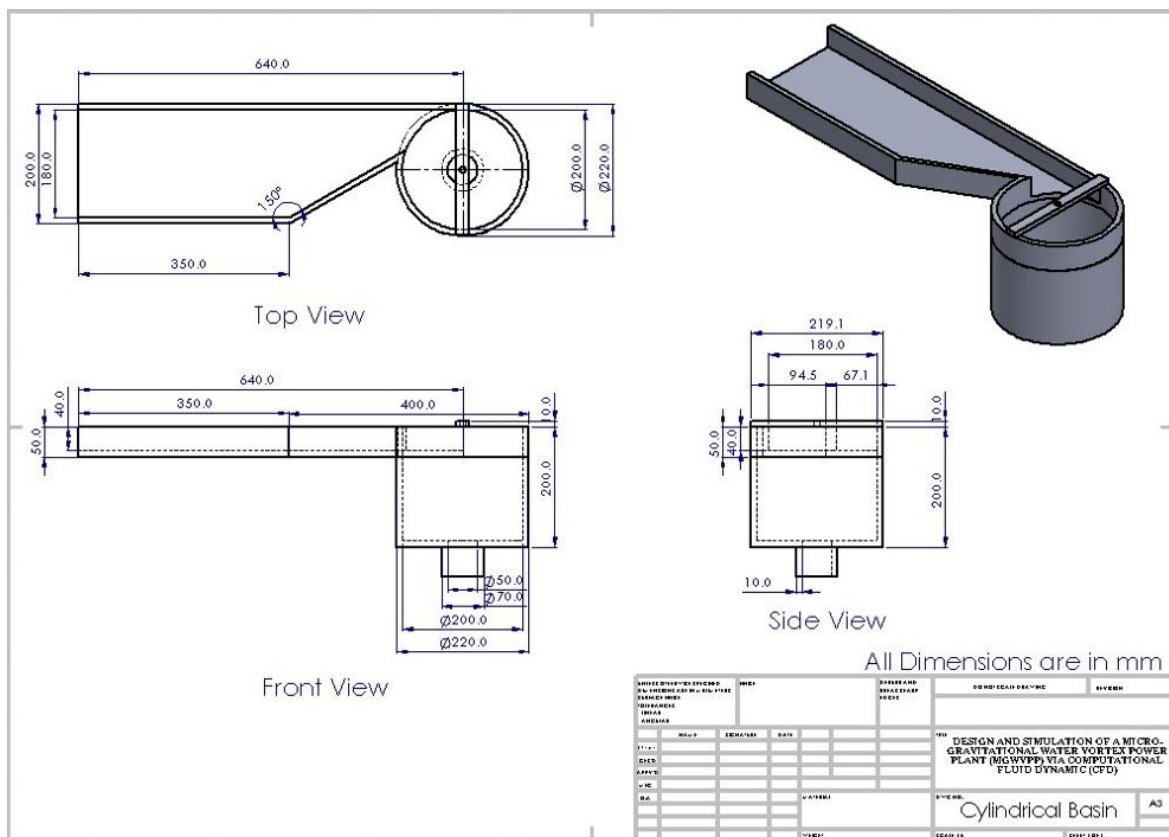


Fig. 2. Cylindrical basin model based on actual size dimensions

3.2 CAD of the Turbine Blades

Kaplan turbine was selected to investigate the MGWVPP. The design includes a rotor with 5 blades, connected to a shaft. The MGWVPP was experimented with 3 variations of curved angle i.e. 140°, 150° and 160°, as shown in Figure 3(a)-(d). The remaining dimensions of the turbine are the same: radius of curvature 50 mm, blade length, 80 mm and blade thickness 8 mm. Figure 4 shows a sample of the 3D printed turbine blades.

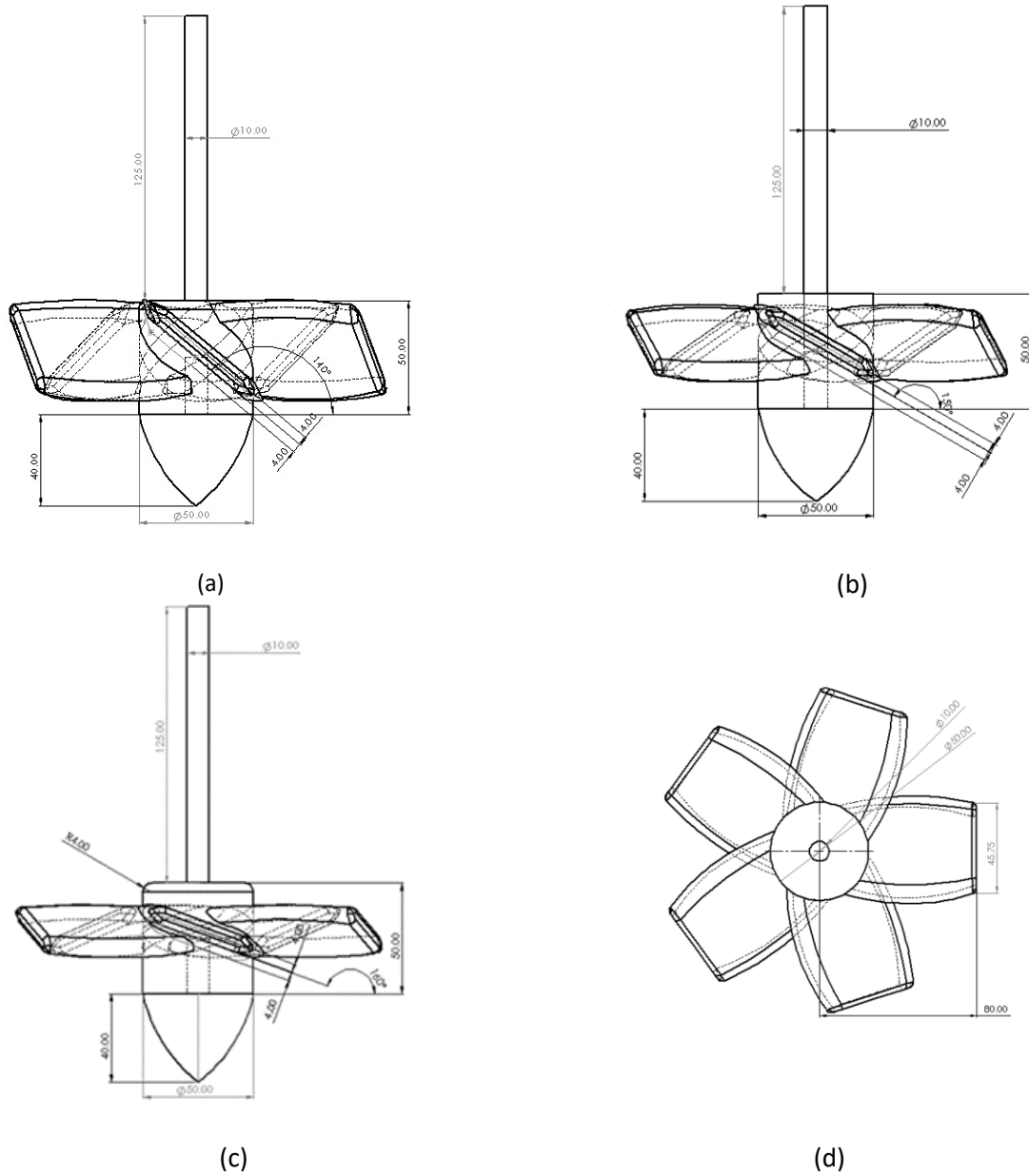


Fig. 3. The view of blade (a) Side view; curved angle 140° (b) Side view; curved angle 150° (c) Side view; curved angle 160° (d) Top view (based on curved angle 150°)



Fig. 4. Sample of a 3D printed turbine blades

3.3 CFD Simulation

The cylindrical basin and turbine models were imported part-by-part from Solidworks to Ansys Design Modeller. Meshing was done using the tetrahedral mesh elements in Ansys Fluent. To analyse the basin and the blades, different simulation parameters and boundary conditions were used. For the basin, where there is no blade domain, the boundary conditions were applied to the basin domain only. Since the air-core vortex is formed due to the air-water interface, two fluids are defined for the simulation: air and water. Built-in fluid models are utilized for both fluids. The properties of water and air, such as density and viscosity, are considered at a temperature of 25°C and a pressure of 1 atm. As the entire runner is not fully immersed in water, air is present inside the runner in the regions that are not submerged.

A multiphase simulation is required to accurately simulate the vortex and the turbine behaviour. In the production of air-core vortices, buoyancy plays a vital role. Therefore, the simulation includes the consideration of buoyancy effects. This accounts for the influence of the density differences between air and water on the flow patterns and the formation of the vortex. Overall, the simulation setup involves defining the two fluids (air and water), their properties, applying appropriate boundary conditions, utilizing multiphase simulation techniques, and incorporating buoyancy effects to accurately model the air-core vortex and turbine behaviour.

Several assumptions are made regarding the fluid flow in this project which include the following:

- i. The fluid is ideal with a steady flow.
- ii. The fluid's characteristics remain constant.
- iii. The linear connection between shear stress and shear rate as well as a constant molecular viscosity define the Newtonian fluid.
- iv. The non-slip condition will be used in the phase, where the wall is assumed to be adiabatic.

The turbulence model selected for this project's simulation is the k - ϵ model. This model was used to explain fluid flow behaviour and deliver more accurate findings for the water flow in an enclosed area. The two-equation model transport for the turbulence kinetic energy (k) and its dissipation rate (ϵ) is the foundation of the conventional k - ϵ model.

The governing equations used for the water vortex assumes a steady, incompressible, viscous, and turbulent flow. The continuity equation and the Navier-Stokes equations, as follows [3]:

$$\frac{\partial V_r}{\partial r} + \frac{\partial V_z}{\partial z} + \frac{V_r}{r} = 0 \quad (1)$$

$$V_r \frac{\partial V_\theta}{\partial r} + V_z \frac{\partial V_\theta}{\partial z} - \frac{V_\theta V_r}{r} = \nu \left(\frac{\partial^2 V_\theta}{\partial r^2} + \frac{\partial V_\theta}{r \partial r} - \frac{V_\theta}{r^2} + \frac{\partial^2 V_\theta}{\partial z^2} \right) \quad (2)$$

$$V_r \frac{\partial V_r}{\partial r} + V_z \frac{\partial V_r}{\partial z} - \frac{V_\theta^2}{r} + \frac{\partial \rho}{\rho \partial r} = \nu \left(\frac{\partial^2 V_r}{\partial r^2} + \frac{\partial V_r}{r \partial r} - \frac{V_r}{r^2} + \frac{\partial^2 V_r}{\partial z^2} \right) \quad (3)$$

$$V_r \frac{\partial V_z}{\partial r} + V_z \frac{\partial V_z}{\partial z} + \frac{\partial \rho}{\rho \partial z} = g + \nu \left(\frac{\partial^2 V_z}{\partial r^2} + \frac{\partial V_z}{r \partial r} + \frac{\partial^2 V_r}{\partial z^2} \right) \quad (4)$$

where, V_r = radial velocity; V_θ = tangential velocity; V_z = axial velocity; g = gravitational acceleration; ν = kinematic viscosity; ρ = density of the fluid.

3.4 Calculation of Performance based on Simulation

Data collected from CFD simulation are velocity on rotational area, velocity on turbine blade, torque and flow rate. Data collected were used to calculate the power efficiency of the whole system. The purpose of performance evaluation in this study is to evaluate and compare the performance of all 3 blade angles design. Also, simulation results of the scaled-down model were compared with experiment results. To compare and validate designs, turbine efficiency was calculated.

From the simulation result, flow rate was used to calculate power input while torque as used to calculate power output. The input power, P_{in} and output power, P_{out} and the turbine efficiency are calculated as follows:

$$P_{in} = \rho g Q H \quad (\text{in watt}) \quad (5)$$

where ρ = density of the fluid (in kg/m³); g = gravitational constant; Q = volumetric flow rate of the fluid (in m³/s); H = Height difference across the turbine (m). The power input is influenced by the height of the vortex and the water flow rate [8].

$$P_{out} = T \omega \quad (\text{in watt}) \quad (6)$$

where T =torque (Nm); ω = angular velocity (rads/s)

Hence, the turbine efficiency, η was calculated as,

$$\eta = \frac{P_{out}}{P_{in}} \times 100\% \quad (7)$$

3.5 Experimental Data Collection

The prototype was assembled and installed with a generator to operate the system, as shown in Figure 5. The voltage and current produced by the prototype were measured using a digital multimeter. The multimeter as connected to the generator and 20 sample measurements were recorded for each run. The power output, P_{out} was calculated based on the experimental data collection as,

$$P_{out} = VI \quad (\text{unit in watts}) \quad (8)$$

where V is voltage and I is current. Figure 6 shows the schematic diagram of the experimental set-up.

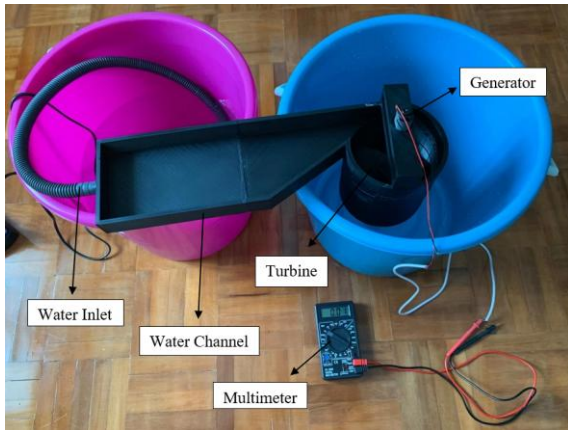


Fig. 5. Assembly of prototype for experimental data collection

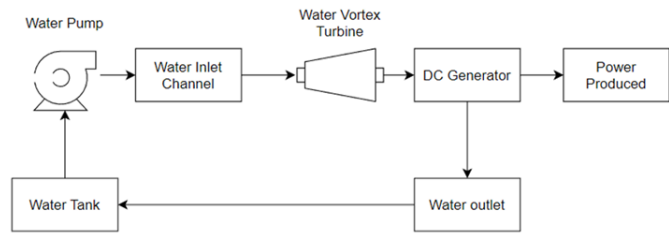


Fig. 6. Schematic diagram of the experimental set-up

4. Results and Discussion

4.1 Simulation Results based on Actual Size

Results obtained includes streamline of the flow, velocity on rotational area, velocity on turbine blade, torque, and flow rate of water. Observing the streamlines in Ansys Fluent allows for the identification of various flow patterns within the domain, including vortex structures, separation zones, recirculation regions, and areas of high or low velocity. It is important to pay attention to the overall flow behaviour and the interaction of streamlines with boundaries or obstacles. This analysis provides valuable insights into the flow characteristics. Besides that, the flow rate and torque are used to calculate the power input and power output by using the equation mentioned in

4.1.1 Flow simulation

Figure 7, 8 and 9 show the flow pattern, velocity and vortex structures in the rotatory domain for blade angle 140° , 150° and 160° , respectively. For blade angle 140° shown in Figure (a) and (b), the rotational domain exhibits the highest intensity of vortex structures. A prominent vortex structure is formed at the bottom of the turbine, as indicated by the presence of green-coloured streamlines (velocity 0.8698 m/s). Significant swirling motion and rotational flow was observed in this region. Moreover, the surface of the turbine displays the maximum velocity streamline, which reaches a value of 1.74 m/s. This indicates that the fluid particles on the surface of the turbine have the highest velocity and momentum among all the observed streamlines. Similar streamlines profiles were observed for blade angles 150° and 160° , with each recorded maximum velocity on the turbine surface at 1.736 m/s and 1.735 m/s. However, observing the colour of the streamlines on the bottom half region of the cylindrical basin of each design (see Figure 7(b), 8(b) and 9(b)), the green-coloured streamline for blade angle 140° indicates higher velocity, while the “closer to blue” steamlines colour for blade angles 150° and 160° indicate lower velocities.

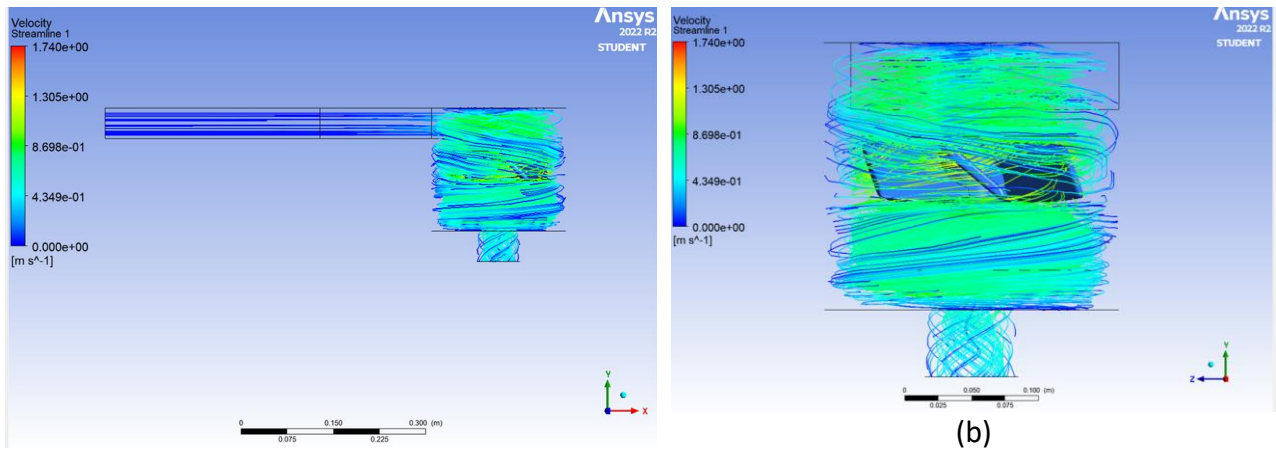


Fig. 7. Streamline velocity for blade angle 140° (a) front view, and (b) side view

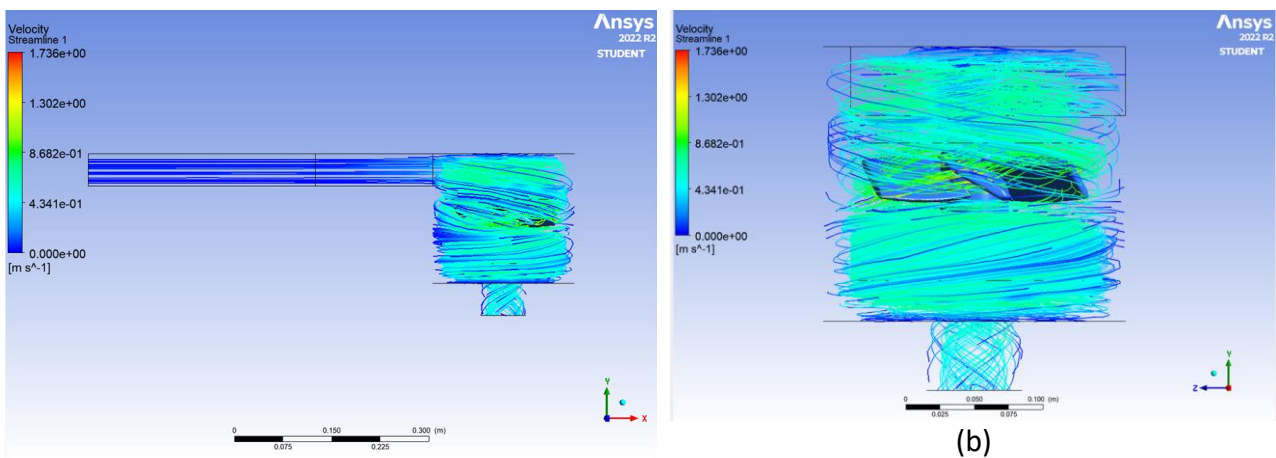


Fig. 8. Streamline velocity for blade angle 150° (a) front view, and (b) side view

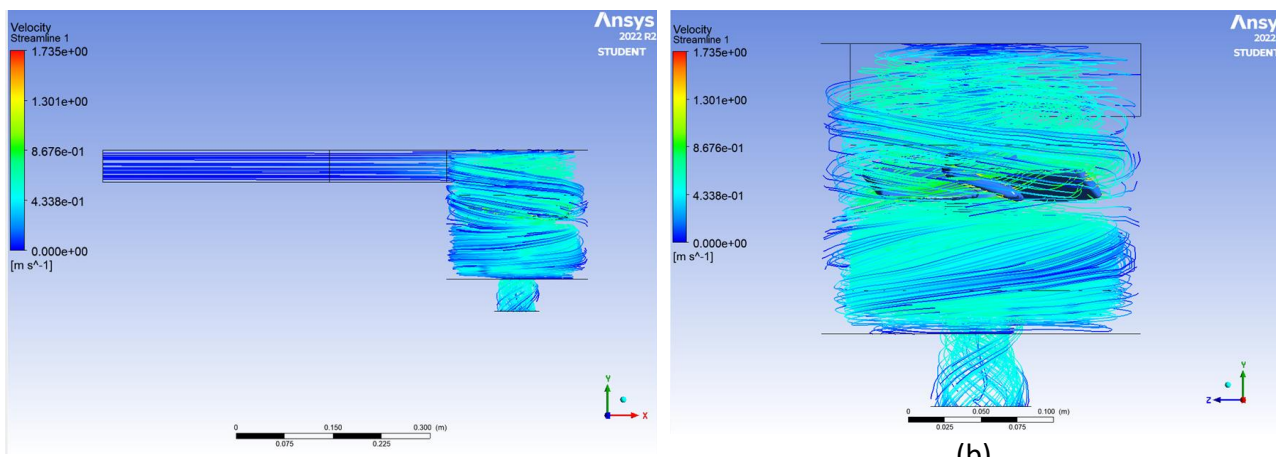


Fig. 9. Streamline velocity for blade angle 160° (a) front view, and (b) side view

4.1.2 Calculation of turbine efficiency

Water is used as the working fluid and is considered to have an incompressible fluid density and viscosity of 997 kg/m^3 and $0.00089 \text{ kgm}^{-1}\text{s}^{-1}$, respectively. The fluid flow's starting mean velocity is

set at 0.1 m/s and the rotation speed was set at 200 rev/min. To compare designs, turbine efficiency was calculated using Eq. (5), (6) and (7). Table 2 and Figure 10 summarise the simulation data and power calculations.

Table 2

Simulation data and power calculations of actual size models

Blade angle	Velocity on rotational area (m/s)	Torque (Nm)	Flow rate (m ³ /s)	Power in (W)	Power out (W)	Efficiency (%)	Percentage difference
140°	0.97017	0.11474	0.003679	2.51906	2.40313	95.40	-
150°	0.83981	0.06965	0.003144	2.15267	1.45884	67.77	28.96%
160°	0.75193	0.03587	0.002616	1.79102	0.75122	41.94	38.11%

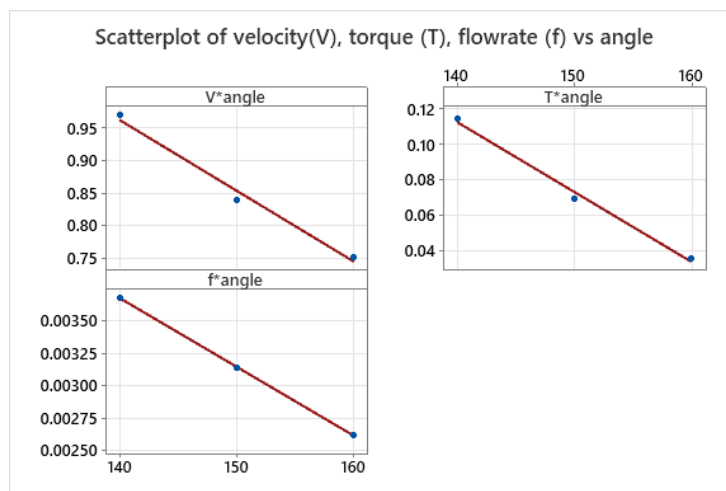


Fig. 10. Scatterplot of velocity, torque and flow rate against blade angle

Figure 10 shows that velocity, torque and flow rate decline in linear proportion as blade angle increases from 140° to 160°. With blade angle at 140°, the velocity, torque and flow rate is at 0.97 m/s, 0.115 Nm and 0.00368, respectively. Efficiency of the MGWVPP turbine with blade angle 140° is estimated at 95.40% and reduces to 67.77% and 41.94%, respectively for 150° and 160° angle. The percentage difference in efficiency for changes in angle from 140° to 150° is 28.96% and from 150° to 160° is 38.11%.

4.2 Simulation Results based on Scaled-down Size

The scaled-down simulation was used to validate experimental results, with assumptions of steady flow conditions and slip-free environment. Water was selected as the working fluid, with properties of incompressible fluid density of 997 kg/m³ and viscosity of 0.00089 kgm⁻¹s⁻¹, respectively. Simulation was initialised with a mean flow rate of 0.0004166667 m³/s and a rotational speed of 200 rev/min. To compare designs, turbine efficiency was calculated using Eq. (5), (6) and (7). Table 3 summarises the simulation data and power calculations.

Table 3
 Simulation data and power calculations of scaled-down models

Blade angle	Velocity on rotational area (m/s)	Torque (Nm)	Flow rate (m ³ /s)	Power in (W)	Power out (W)	Efficiency (%)	Percentage difference
140°	0.50505	0.000829	0.0004167	0.12226	0.01562	12.78	-
150°	0.46035	0.000525	0.0004167	0.12226	0.00989	8.09	36.70%
160°	0.42918	0.000341	0.0004167	0.12226	0.00643	5.26	34.98%

As shown in Table 3, the decreasing turbine efficiency trend for the scaled-down models are similar to the actual size. Percentage difference in efficiency for changes in angle from 140° to 150° and from 150° to 160° is 36.7% and 34.98% respectively, which is also consistent with the simulation results for the actual size model. Due to the small dimensions, no changes in flow rate, thus constant power input for all blade angles. It was noted that the prototype-sized MGWVPP are inefficient with the highest plant efficiency at 12.7% for blade angle designed at 140°. As stated before, the motivation of simulating a scaled-down model is to compare results with data collected from experimental work.

4.3 Experimental Results

In experimental work, 20 measurements of voltage and current for each blade angle design were collected. Boxplots shown in Figure 11 and 12 summarise the results. For voltage, the mean values were 0.0985 V, 0.087 V and 0.0685 V, for blade angles 140°, 150° and 160°, respectively. For current, the mean values were 0.115 A, 0.0976 A and 0.08965 A for blade angles 140°, 150° and 160°, respectively. The results show that, as the blade angle increases from 140° to 160°, voltage and current decreases.

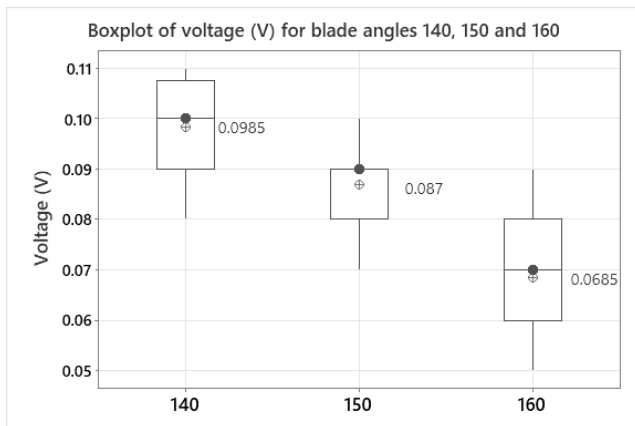


Fig. 11. Boxplot of voltage (V) for blade angles 140°, 150° and 160°

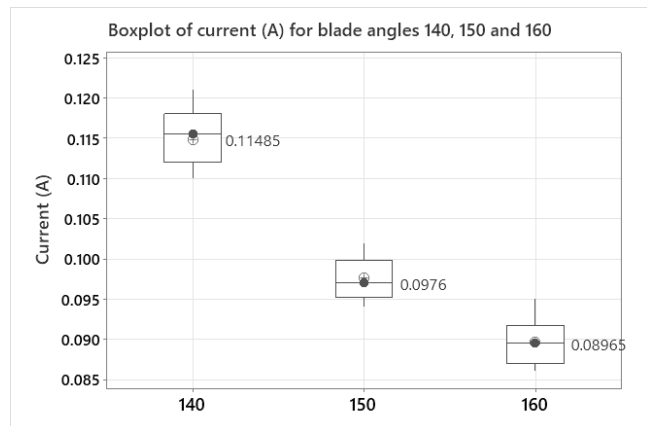


Fig. 12. Boxplot of current (A) for blade angles 140°, 150° and 160°

Consistent with the simulation results, blade angle 140° produces the highest power output. Table 4 summarises the power output based on voltage and current mean values obtained from the experimental work, calculated using Eq. (8), compared to power output based on simulation results. The percentage difference in power output was calculated by taking the simulation result as baseline, as follows. Figure 13 shows the comparison of power output estimated from experiment and simulation.

$$\text{Percentage difference, } \Delta = \left| \frac{\text{Simulation result} - \text{Experimental result}}{\text{Simulation result}} \right| \times 100\% \quad (9)$$

Table 4

Comparison of power output – simulation results (scaled-down) and experimental results

Blade angle	Experiment			Simulation	Percentage difference (%)
	Voltage (V)	Current (A)	Power output (W)	Power output (W)	
140	0.0985	0.11485	0.01131	0.01562	27.6%
150	0.087	0.0976	0.00849	0.00989	14.1%
160	0.0685	0.08965	0.00614	0.00643	4.5%

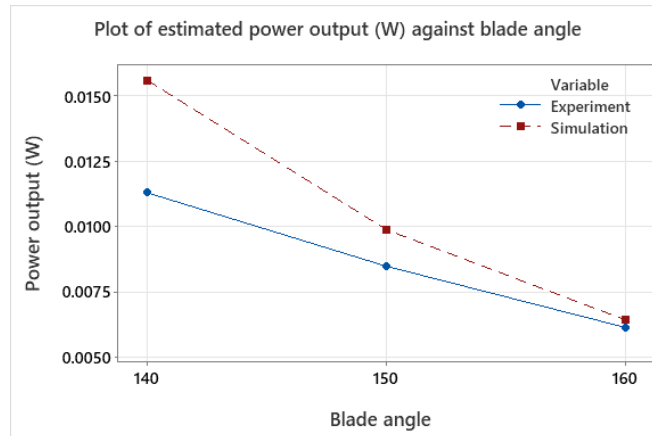


Fig. 13. Comparison of power output estimated from experiment and simulation

From Table 4, it can be stated that the relatively low percentage difference (< 30%) in estimated power output computed from the experimental data collected using the 3D printed turbine and cylindrical basin and the calculated power output from the scaled-down simulation verified the experimental results.

4.4 Discussion of Results

Based on simulation and experimental results, a MGWVPP with cylindrical basin and Kaplan turbine with 5 blades inclined at 140° angle demonstrated best performance compared to the 150° and 160° variants. Observation on fluid simulation showed that the fluid within the rotational domain experiences the highest degree of swirling motion with the 140-degree blade angle, as it indicates the highest intensity of vortex structure. The decrease in torque values from 140° to 160° blade angle is due to the gap between the blades. The 160° blade angle has the smallest gap between the blades which leading to an increased velocity of water passing through it and resulting in the formation of a whirlpool on the discharge side. This whirlpool causes obstructed water flow, known as the blocking effect phenomenon, which hinders the smooth movement of water and ultimately contributes to a decrease in torque values generated by the turbine [1].

Numerical simulations predict higher power output compared to the experimental results for all three blade angles. This may be due to various factors, such as uncertainties in the simulation models, approximations made during calculations, and discrepancies between the experimental setup and the modelled conditions. However, the power efficiency obtained from numerical and experimental are acceptable in the range of maximum efficiency of gravitational water vortex power plant.

According to [14], the turbine in the water free vortex turbine system achieved the maximum power output of 14.5 watts, and its efficiency was measured to be 35.92%.

5. Conclusion

The primary aim of this study was to design and investigate the performance of micro-gravitational water vortex power plant (MGWVPP) for 3 different Kaplan turbine blade angles i.e. 140°, 150° and 160°. Design and simulation of Kaplan turbine blade angles were done using SolidWorks and Ansys. CFD simulation as conducted using Ansys Fluent. Experimental results were obtained using an assembly of prototype-sized MGWVPP. The cylindrical basin and turbines were 3D-printed using Creality Ender 5 Plus 3D printer. Results obtained from simulations and experiment consistently showed a Kaplan turbine with curved blade angle at 140° showed the best performance. Based on the simulation results, for a proposed actual-sized MGWVPP with cylindrical basin diameter × height of 220 mm × 200 m and a Kaplan turbine with 5-blade curved angle at 140°, the power generation system is capable of producing 2.4 W at more than 90% efficiency. A scaled-down prototype-sized system with cylindrical basin diameter × height of 110 mm × 100 m expectedly produced lower power at 0.011 W (from experiment) and 0.016 W (from simulation). For future work, similar simulation study can utilise a higher quality mesh in Ansys, as the student version Ansys used in this research was limited. The research can also be extended by investigating other blade profiles in various basin geometries and shape. Fabrication of the turbine prototype can also be improved by manufacturing a smoother and higher quality surface.

Acknowledgement

This research was conducted at Universiti Malaysia Sarawak without external funding. We extend our gratitude to the university for its essential support and resources. The university's facilities, expertise, and academic environment were instrumental in the success of our project.

References

- [1] Brijkishore, Ruchi Khare, and Vishnu Prasad. "Performance evaluation of Kaplan turbine with different runner solidity using CFD." In *Advanced Engineering Optimization Through Intelligent Techniques: Select Proceedings of AEOTIT 2018*, pp. 757-767. Singapore: Springer Singapore, 2019. https://doi.org/10.1007/978-981-13-8196-6_67
- [2] Chan, Zin Mar, and Zar Ni Aung. "Design calculation of Kaplan Turbine Runner Blade for 15kw Micro Hydropower Plant." *International Journal for Advance Research and Development* 5, no. 4 (2020): 14-16.
- [3] Dhakal, Sagar, Ashesh B. Timilsina, Rabin Dhakal, Dinesh Fuyal, Tri R. Bajracharya, Hari P. Pandit, Nagendra Amatya, and Amrit M. Nakarmi. "Comparison of cylindrical and conical basins with optimum position of runner: Gravitational water vortex power plant." *Renewable and Sustainable Energy Reviews* 48 (2015): 662-669. <https://doi.org/10.1016/j.rser.2015.04.030>
- [4] Kueh, Tze Cheng, Shiao Lin Beh, Dirk Rilling, and Yongson Ooi. "Numerical analysis of water vortex formation for the water vortex power plant." *International Journal of Innovation, Management and Technology* 5, no. 2 (2014): 111.
- [5] Maika, Nosare, Wenxian Lin, and Mehdi Khatamifar. "A review of gravitational water vortex hydro turbine systems for hydropower generation." *Energies* 16, no. 14 (2023): 5394. <https://doi.org/10.3390/en16145394>
- [6] Jorge Morales Pedraza. 2022. Chapter 2 - The use of hydropower for electricity generation. In *Non-Conventional Energy in North America*, Jorge Morales Pedraza (ed.). Elsevier, 89-135. <https://doi.org/10.1016/B978-0-12-823440-2.00010-X>
- [7] Nishi, Yasuyuki, Ryouta Suzuo, Daichi Sukemori, and Terumi Inagaki. "Loss analysis of gravitation vortex type water turbine and influence of flow rate on the turbine's performance." *Renewable Energy* 155 (2020): 1103-1117. <https://doi.org/10.1016/j.renene.2020.03.186>
- [8] Power, Christine, Aonghus McNabola, and Paul Coughlan. "A parametric experimental investigation of the operating conditions of gravitational vortex hydropower (GVHP)." *Journal of Clean Energy Technologies* 4, no. 2 (2016): 112-119. <https://doi.org/10.7763/JOCET.2016.V4.263>

- [9] Rahman, M. M., J. H. Tan, M. T. Fadzlita, and AR Wan Khairul Muzammil. "A review on the development of gravitational water vortex power plant as alternative renewable energy resources." In *IOP Conference Series: Materials Science and Engineering*, vol. 217, no. 1, p. 012007. IOP Publishing, 2017. <https://doi.org/10.1088/1757-899X/217/1/012007>
- [10] Alejandro Ruiz Sánchez, Jorge Andrés Sierra Del Rio, Angie Judith Guevara Muñoz, and José Alejandro Posada Montoya. "Numerical and Experimental Evaluation of Concave and Convex Designs for Gravitational Water Vortex Turbine." *J. Adv. Res. Fluid Mech. Therm. Sc.* 64, no. 1 (2020): 160-172.
- [11] Shabara, H. M., O. B. Yaakob, Yasser M. Ahmed, and A. H. Elbatran. "CFD simulation of water gravitation vortex pool flow for mini hydropower plants." *Jurnal Teknologi (Sciences & Engineering)* 74, no. 5 (2015). <https://doi.org/10.11113/jt.v74.4645>
- [12] Sharif, A., M. Siddiqi, and R. Muhammad. "Novel runner configuration of a gravitational water vortex power plant for micro hydropower generation." *Journal of Engineering and Applied Sciences* 39, no. 1 (2020): 87-93. <https://doi.org/10.17582/journal.jeas/39.1.87.93>
- [13] Sritram, P., and R. Suntivarakorn. "The effects of blade number and turbine baffle plates on the efficiency of free-vortex water turbines." In *IOP Conference Series: Earth and Environmental Science*, vol. 257, no. 1, p. 012040. IOP Publishing, 2019. <https://doi.org/10.1088/1755-1315/257/1/012040>
- [14] Sritram, Piyawat, and Ratchaphon Suntivarakorn. "Comparative study of small hydropower turbine efficiency at low head water." *Energy Procedia* 138 (2017): 646-650. <https://doi.org/10.1016/j.egypro.2017.10.181>
- [15] Tamiri, F. M., M. A. Ismail, and W. K. Muzammil. "Low head micro hydro systems for rural electrification." In *IOP Conference Series: Materials Science and Engineering*, vol. 834, no. 1, p. 012041. IOP Publishing, 2020. <https://doi.org/10.1088/1757-899X/834/1/012041>
- [16] Wanchat, Sujate, and Ratchaphon Suntivarakorn. "Preliminary design of a vortex pool for electrical generation." *Advanced Science Letters* 13, no. 1 (2012): 173-177. <https://doi.org/10.1166/asl.2012.3855>